IOP Publishing Journal of Physics D: Applied Physics
J. Phys. D: Appl. Phys. **47** (2014) 435002 (9pp) doi:10.1088/0022-3727/47/43/435002

# Unravelling the effect of $SrTiO_3$ antiferrodistortive phase transition on the magnetic properties of $La_{0.7}Sr_{0.3}MnO_3$ thin films

**D A Mota[1], Y Romaguera Barcelay[1], A M R Senos[2], C M Fernandes[2], P B Tavares[3], I T Gomes[4], P Sá[4], L Fernandes[4], B G Almeida[4], F Figueiras[5], P Mirzadeh Vaghefi[5], V S Amaral[5], A Almeida[1], J Pérez de la Cruz[1] and J Agostinho Moreira[1]**

[1] IFIMUP and IN-Institute of Nanoscience and Nanotechnology, Departamento de Física e Astronomia da Faculdade de Ciências da Universidade do Porto. Rua do Campo Alegre, 687, 4169-007 Porto, Portugal
[2] Department of Materials and Ceramics Engineering, CICECO, University of Aveiro, 3810-193 Aveiro, Portugal
[3] Centro de Química—Vila Real, Universidade de Trás-os-Montes e Alto Douro, Apartado 1013, 5001-801 Vila Real, Portugal
[4] Centro de Física. Universidade do Minho, P-4710-057 Braga, Portugal
[5] Department of Physics and CICECO, University of Aveiro, 3810-193 Aveiro, Portugal

E-mail: jamoreir@fc.up.pt

Received 19 June 2014, revised 19 August 2014
Accepted for publication 29 August 2014
Published 3 October 2014

**Abstract**

Epitaxial $La_{0.7}Sr_{0.3}MnO_3$ (LSMO) thin films, with different thicknesses ranging from 20 to 330 nm, were deposited on (1 0 0)-oriented strontium titanate (STO) substrates by pulsed laser deposition, with their structure and morphology characterized at room temperature. The magnetic and electric transport properties of the as-processed thin films reveal an abnormal behaviour in the temperature dependent magnetization $M(T)$ below the antiferrodistortive STO phase transition ($T_{STO}$), and also an anomaly in the magnetoresistance and electrical resistivity close to the same temperature. Films with thickness ≤100 nm show an in-excess magnetization and pronounced changes in the coercivity due to the interface-mediated magnetoelastic coupling with antiferrodistortive domain wall movement occurring below $T_{STO}$. However, in thicker LSMO thin films, an in-defect magnetization is observed. This reversed behaviour can be understood with the emergence in the upper layer of the film, of a columnar structure needed to relax the elastic energy stored in the film, which leads to randomly oriented magnetic domain reconstructions. For enough high-applied magnetic fields, as thermodynamic equilibrium is reached, a full suppression of the anomalous magnetization occurs, wherein the temperature dependence of the magnetization starts to follow the expected Brillouin behaviour.

Keywords: thin films, magnetic domain reconstruction, interface-mediated coupling, magnetoelasticity

(Some figures may appear in colour only in the online journal)

## 1. Introduction

Rare-earth manganite compounds exhibit a strong coupling between their electronic, spin and structural degrees of freedom [1, 2]. Due to this coupling, these materials show a rich variety of effects when a change in one of the degrees of freedom induces a response in another [2–4]. An interesting case is found in compounds revealing an interplay between

 

the lattice and the magnetic response, through either spin-phonon or spin-lattice coupling [5–7]. In such materials, the super-exchange interactions, determining the magnetic and electric properties, are found to be strongly dependent on both the Mn-O and the tilting of the $MnO_6$ octahedra [8, 9]. Deformation and tilting of the $MnO_6$ octahedra can stabilize the different magnetic structure and alter electron transfer. The change in Mn-O-Mn bond angles results in variation off the double-exchange transfer integral and thus directly affects both transport and magnetic properties [10]. Due to the high sensitivity of the magnetism on the lattice distortion, colossal magnetoresistance $La_{0.7}Sr_{0.3}MnO_3$ (LSMO) epitaxial thin films are good candidates to probe the effects of structural changes on the magnetotransport and magnetic properties. The strain induced by the lattice mismatch between the LSMO film and the substrate changes both the Mn-O bond lengths and the Mn-O-Mn bond angles [10, 11]. This feature turns their structural, transport and magnetic properties to be strongly dependent on the substrate characteristics.

Strontium titanate (STO) is a cubic perovskite material at room temperature, widely used as the substrate for epitaxial growth of manganite films, inducing biaxial strain, either compressive or tensile, depending on the growing thin film. STO undergoes a structural phase transition into an antiferrodistortive phase at $T_{STO} = 105$ K, with tetragonal symmetry [12]. This phase transition is driven by an unstable lattice mode of the Brillouin zone boundary, associated with the rotation of the $TiO_6$ octahedra around a former cubic axis, producing an expansion of the unit cell in the tetragonal *c*-axis, and a contraction in the two other perpendicular directions [12]. The change in lattice parameter at $T_{STO}$ is on the order of 0.1% [12].

Several studies on $La_{1-x}Sr_xMnO_3$ epitaxial thin films, with $x = 0.20$–$0.47$, processed onto oriented (1 0 0)-STO substrates, were published, and the effect of the STO antiferrodistortive phase transition on the magnetic and transport properties has been the subject of several reports [13–16]. However, no unique interpretation of the experimental results has been reached. According to Segal *et al* [13], the electrical resistivity cusp and magnetization dip observed near $T_{STO}$ on $La_{0.53}Sr_{0.47}MnO_3$ ultra-thin films (11 unit cells) results from an evanescent cross-interface coupling between the charge carriers in the film and the soft phonon in the STO, mediated through linked oxygen octahedral motions. The motions of the $TiO_6$ octahedra couple to the $MnO_6$ inducing both static and dynamic changes in their configuration [13]. According to these authors, the static effect appears only below $T_{STO}$ and does not explain the anomalous temperature behaviour of both resistivity and magnetization. In order to account for these anomalies, a dynamical coupling was assumed [13]. Near $T_{STO}$, the correlation length in STO diverges and the oxygen motions in the interfacial $La_{0.53}Sr_{0.47}MnO_3$ layer become correlated with the resistivity and magnetization anomalies observed in the film. So, the soft phonons extend into the $La_{0.53}Sr_{0.47}MnO_3$ layer and couple with magnon modes. However, the penetration depth of these soft phonons was estimated to be just a few (2–3) atomic layers of the film; as such, this effect should not be observed in thicker films [13].

More recently, Pesquera *et al* [14] reported an experimental study of the dc and ac magnetic properties in $La_{0.67}Sr_{0.33}MnO_3$ thin films (26 and 220 nm thickness) prepared onto (1 0 0)-oriented STO substrates. In order to explain the anomalous magnetic responses at low ac-magnetic field and at high dc-field, even in thicker films, magnetic domain pattern reconstruction and creation of regions within the magnetically soft LSMO with enhanced magnetic anisotropy were proposed as two distinct mechanisms, triggered by the STO phase transition [14]. These authors refute the dynamical coupling with the soft phonon assumed in an earlier work [13], as a similar anomalous temperature behaviour of the magnetization is also observed in the thicker films [14]. It is interesting to stress that the LSMO films used in both works have different compositions. This may prevent a straight comparison between the results obtained, since their physical properties may be different, as it can be suggested from the (%Sr, T) phase diagram [17].

Other experimental reports regarding the magnetic properties of LSMO thin films on STO substrates were published. Ziese *et al* [15] reported an experimental study of ac magnetic susceptibility in $La_{0.7}Sr_{0.3}MnO3$ thin films, deposited in single terminated (1 0 0)-STO substrates, focused on very thin films (5–40 nm). According to these authors, the structural transition of the STO substrate induces a magnetic phase transition in the manganite films, due to magnetoelastic coupling, associated with magnetic regions with different coercive fields [15]. However, the aforementioned report was focused on the temperature dependence of the magnetic properties in fully strained thin films. Egilmez *et al* [16] reported an experimental study of the resistivity of $La_{0.8}Sr_{0.2}MnO_3$ ultrathin thin films, grown on STO substrate and bearing thicknesses between 9 and 150 nm, prepared through rf magnetron sputtering. They reported the observation of satellite peaks in the temperature dependence of the temperature coefficient of resistivity (TCR) at temperatures around 105 K, triggered by the cubic-to-tetragonal structural phase transition of STO. However, no change in the electrical transport properties has been detected at $T_{STO}$.

Although the extensive study of the effect of the structural phase transition of the STO on the magnetic and transport properties of LSMO thin films on STO oriented substrates, the effect of the pinning of the substrate on the magnetic properties of LSMO thin films, as a function of film thickness and under weak external dc magnetic fields, has not yet been explored. In this work, we present an experimental study of the effect of the domain pattern of the oriented (1 0 0)-STO substrate on the magnetic and electric transport properties of LSMO thin films, as a function of film thickness, ranging between 20 and 300 nm. This work differs from the ones in [13–16] by studying in detail the effect of the structural changes occurring in the substrate at $T_{STO}$ on the magnetic properties of fully strained to relaxed thin films, by performing both $M(T)$ and $M(H)$ measurements and also its dependence with the magnitude of the applied magnetic field.

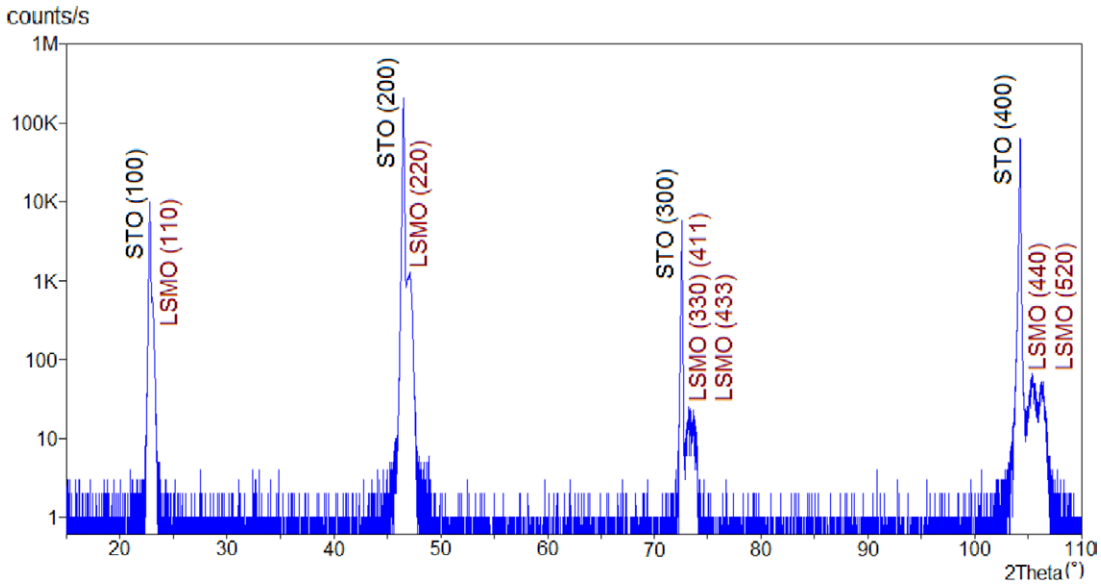


**Figure 1.** X-ray diffraction pattern obtained for the 210 nm LSMO film sample, displaying the respective indexations of the $SrTiO_3$ (STO) substrate to the Cubic *Pm-3m* (2 1 1) symmetry group, and of the LSMO thin film to the Rhomboedric *R-3c* (1 6 7) pseudomorphic phase.

## 2. Experimental

High quality ceramic LSMO targets were prepared by the solid-state method [18]. Epitaxial LSMO thin films, with thicknesses between 20 and 330 nm, were grown on single crystalline oriented (1 0 0)-STO substrates by pulsed laser deposition. The depositions were carried out with a KrF excimer laser (wavelength $\lambda$ = 248 nm), at a fluence of 1.5 J cm$^{-2}$, with a 3 Hz repetition rate and pulse duration of 25 ns. The target-to-substrate distance was kept constant at 5.5 cm during the depositions, which were performed in a pure oxygen atmosphere with 0.8 mbar pressure, and with a substrate temperature of 700 °C. To prevent under-oxidation of the films after deposition, they were cooled down to room temperature at 15 °C min$^{-1}$ in a pure oxygen atmosphere, at room pressure.

Atomic force microscopy (AFM) measurements were performed in a Nanoscope IVa multimode system in the tapping mode using Si tips. Scanning electron microscopy (SEM) measurements were performed in an FEI Quanta 400 FEG ESEM scanning electron microscope operated at 20 kV and with a resolution of 1.5 nm for both surface morphology and film thickness characterization. The film thickness was evaluated by performing SEM measurements in the cross section of the films and confirming it with x-ray reflectometry. High resolution x-ray diffraction (HR-XRD) [19] measurements were performed in an XPERT-PRO Diffractometer, using the main x-ray line: $Cu_{k\alpha 1}$ = 1.5405980 Å through a 4xGe220 Asym. monochromator.

The dc magnetic properties were measured with a Quantum Design MPMS SQUID magnetometer, with the reciprocating sample option along the [1 0 0] in-plane and out-of-plane directions and with a resolution up to $10^{-7}$ emu. Electrical resistivity and magnetoresistance measurements were performed in the temperature ranges 25–300 K and 80–300 K, respectively. In both cases, a standard four probe method was used. A magnetic field of 1 T applied parallel to the electrical current and along the [1 0 0] in-plane direction was used for the magnetoresistance measurements.

Cross-sectional samples were thinned by mechanical polishing to about 100 µm and then ion milled using a JEOL EM-09100 IS ion slicer until electron transparency. HRTEM studies were performed by using an FEI Technai electron microscope operated at 200 kV, with a 0.17 nm spatial resolution.

## 3. Results and discussion

The surface analysis of the 60 nm LSMO thin film, through AFM and SEM, respectively, show a uniform topography, with a root mean square roughness of approximately 1 nm, which is of the same order of magnitude even for scans over 2 × 2 µm$^2$, revealing an almost layer-by-layer growth with some islands nucleation at the surface. The grains, defined by sharp squared crystallites with common alignment of edges, have sizes ranging between 30 and 50 nm. Despite a slight roughness increase with increasing film thickness, similar results, regarding grain shape and grain-size, were ascertained for all the as-processed LSMO thin films.

Figure 1 shows an illustrative x-ray diffraction spectrum obtained for the 210 nm LSMO film. The thin film exhibits a clear preferential growth, following the {1 0 0} orientation of the cubic *Pm-3m* (2 2 1) $SrTiO_3$ substrate. Taking into account the peaks splitting found at higher angles of the spectrogram, the film structure can be indexed to the Rhombohedral *R-3c* (167) space group, which was verified by performing HR-XRD measurements at the most representative allowed reflections. Symmetric pole figures obtained around $2\theta = 22.7°$ and 46.8°, exhibit the respective substrate central reflection from the $(1\,0\,0)_c$ and $(2\,0\,0)_c$ planes, respectively, along with a small adjacent peak arising from the film phase in a narrow direction of $\psi$. Specific details are further revealed through

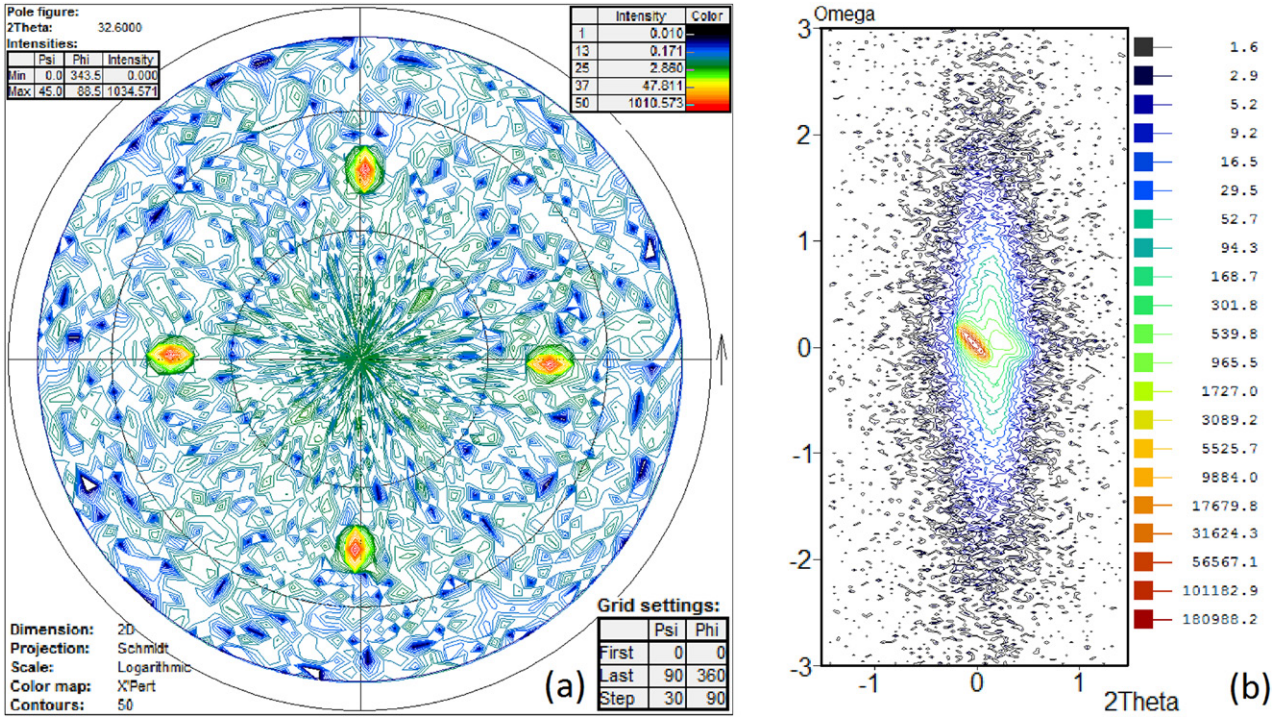


**Figure 2.** 2D asymmetric pole figure at $2\theta = 32.6°$ of the 210 nm LSMO thin film (*a*) and map centred at $2\theta = 46.50°$ and $\Omega = 23.25°$ (*b*).

examples of the asymmetric pole figures and reciprocal space mapping for some representative samples. For the 210 nm LSMO thin film, the HR-XRD results point to approximately 0.44% compressive deformation relative to the conventional bulk form ($\boldsymbol{a}$ = 5.472 Å, $\boldsymbol{\alpha}$ = 60.354°) [20] for the $\boldsymbol{d}(1\,1\,0)_R$ planes. The 2D asymmetric pole figure performed at the most intense reflection ($2\boldsymbol{\theta}$ = 32.60°), shown in figure 2(*a*), suggests some relaxation of $(1\,0\,1)_R$ and $(2\,1\,1)_R$ planes of LSMO film relative to the substrate $(1\,1\,0)_C$ plane, denoted by the four peaks elongation in $\boldsymbol{\psi}$ angle. The $\Omega$ versus $2\boldsymbol{\theta}$ map, shown in figure 2(*b*), centred at $2\boldsymbol{\theta}$ = 46.50° and $\Omega$ = 23.25°, covers the STO $(2\,0\,0)_c$ peak and the $(2\,2\,0)_R$ peak of the LSMO film. The strong spread $\Delta\Omega$ (~2°) of the latter peak, diverging from the substrate peak shape, evidences the existence of a significant mechanical tension, which yields a partial bending of the film planes. Moreover, the elongation of the peak in $\Delta\boldsymbol{\theta}$ (~0.5°) can be associated with $\boldsymbol{d}(2\,2\,0)_R$ plane relaxation across the film growth direction. This relaxation may not be homogeneous as observed by Ranno *et al* [21], and further confirmed by our HRTEM analysis.

For the 60 nm LSMO thin film, the HR-XRD results point to approximately 0.62% compressive deformation of the $(1\,1\,0)_R$ planes family relative to the conventional bulk. In the illustrative 2D asymmetric pole figure (figure 3(*a*)) performed around $2\boldsymbol{\theta}$ = 32.60°, it is possible to observe four typical reflections assigned to planes $(1\,0\,1)_R$ and $(2\,1\,1)_R$ of LSMO film, neighbouring the Bragg reflection assigned to the $(1\,1\,0)_C$ plane of STO substrate. A similar $\boldsymbol{\psi}(d_{hkl})$ is observed through the superposition of reflections, whereas the slight spread in the in-plane $\boldsymbol{\varphi}$ angle can be interpreted as a minor rotation between these planes. The $\Omega$ versus $2\boldsymbol{\theta}$ map, shown in figure 3(*b*), centred at $2\boldsymbol{\theta}$ = 46.50° and $\Omega$ = 23.25°, involves the STO $(2\,0\,0)_C$ peak and a single side peak of the $(2\,2\,0)_R$ LSMO thin film, which closely follows the $2\boldsymbol{\theta}$ and $\Omega$ contours from the cubic substrate. This feature evidences both the high degree of epitaxy and the coherent growth of this film.

Figures 4(*a*) and (*b*) show the magnetization of LSMO films as a function of the applied magnetic field parallel to the film plane, recorded at two different fixed temperatures, above and below $T_{STO}$, for 60 nm and 210 nm film thickness, respectively. These results are illustrative examples of the magnetic response of LSMO films for the various thicknesses of films studied in this work. The LSMO films, whose results are presented in figure 4, show typical ferromagnetic hysteresis loops. The remarkable issue is the large variation of the magnetic coercivity of the 60 nm-thick film between 120 K and 60 K, which evidence the strong effect of the appearance of the antiferrodistortive domains of the STO substrate, below $T_{STO}$, on the coercivity of the LSMO films.

Figure 5 shows the coercive field measured at 60 and 120 K as a function of film thickness. It can be observed that for lower thicknesses (20 and 60 nm), the coercive field measured at 60 K is much larger than the one measured at 120 K. However, the difference between the coercive fields measured at 60 and 120 K decreases as the film thickness increases. Moreover, while the coercive field measured at 120 K seems to be weakly thickness dependent, the coercive field measured at 60 K is strongly thickness dependent. The results shown in figure 5 suggest the existence of a 'critical thickness' close to 100 nm, above which the coercivity difference at the two temperatures is smaller and the effect of the STO phase transition on the magnetic properties is less than in thinner films. In fact, the films with a thickness below 100 nm are clamped to the substrate and are the most sensitive to structural changes of

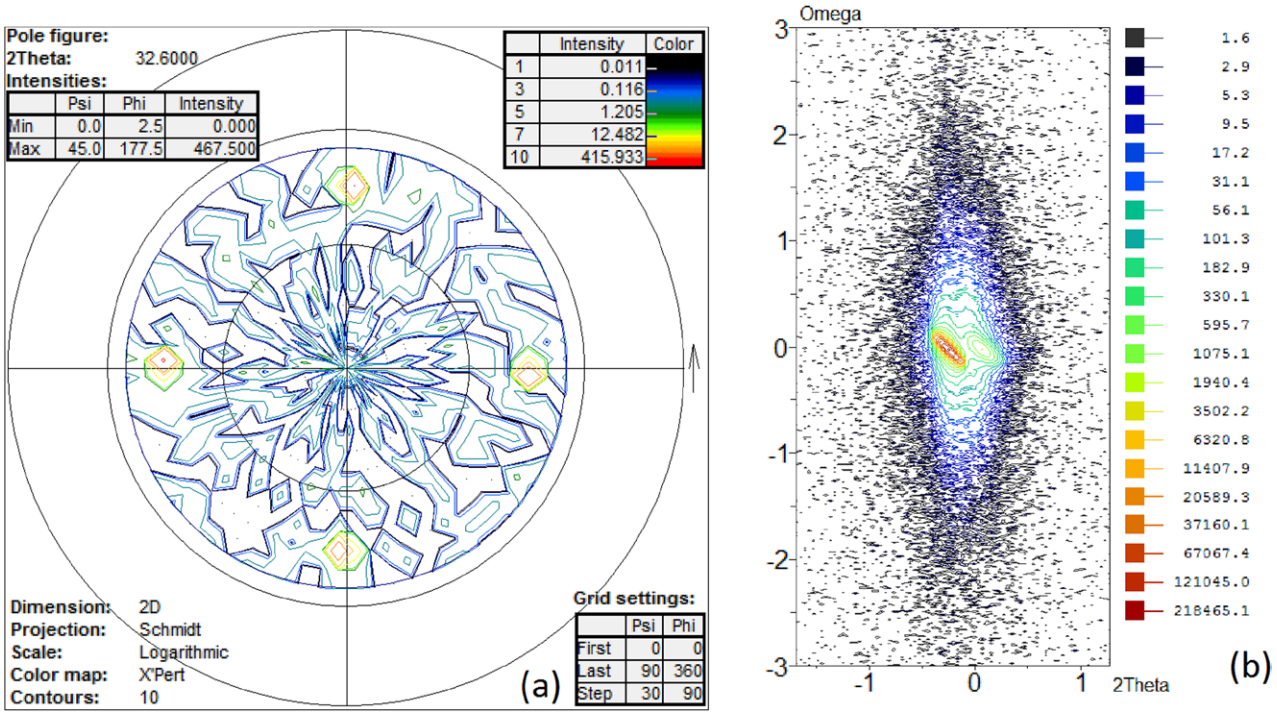


**Figure 3.** 2D asymmetric pole figure at $2\theta = 32.6°$ of the 60 nm LSMO film (*a*) and map centred at $2\theta = 46.50°$ and $\Omega = 23.25°$ (*b*).

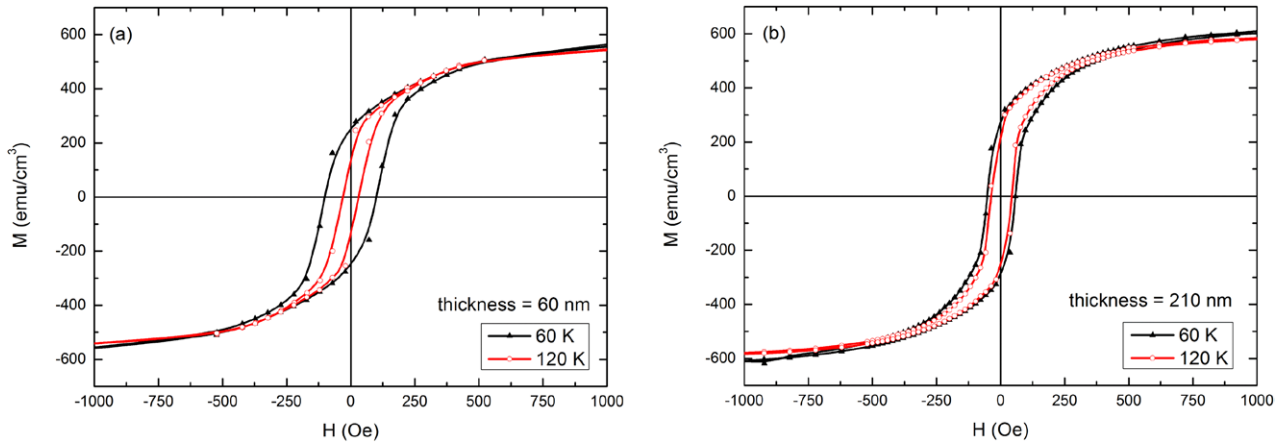


**Figure 4.** Field dependence of magnetization measured at $T = 60$ and 120 K along the [1 0 0] in-plane direction for the 60 nm (*a*) and 210 nm (*b*) LSMO thin film.

the substrate, presenting a remarkable change of coercive field upon cooling through $T_{STO}$. The change in the coercive field results in a stabilization of distinct magnetic domain patterns of the film that depend on the STO antiferrodistortive domain configuration. This effect is more pronounced at remanence or when small magnetic fields are applied to the samples. So, the magnetic properties of such thin films are tailored by the effect of the antiferrodistortive phase transition of the STO substrate, which controls both the coercive field and magnetization. The comparison of $M(H)$ hysteresis loops obtained at 60 and 120 K must be handled carefully, because they have been registered in different physical conditions regarding the STO phase. Looking at the experimental results, a close relation between the structural units of both STO and LSMO film is clearly evident and the structural coupling between STO and film ensured through the STO/LSMO interface is the driving force of the magnetic properties of the LSMO films. In the thinner films, the increase of the coercive field observed at 60 K, relatively to the value at 120 K, is a consequence of the strong pinning of the magnetic domains to the substrate, whose domain pattern changes drastically between these two temperatures. Moreover, the coupling between both structures may influence the dc magnetization on crossing the $T_{STO}$ phase transition. Actually, the impact of the substrate-induced changes is smaller in thicker films due to strain relaxation and possibly to the presence of different layers in thicker films.

Figure 6 shows the HRTEM cross-section of a 330 nm thick film. The existence of two different layers can be distinctly observed; one with a thickness close to 100 nm, wherein the film grows epitaxially and coherently to the STO

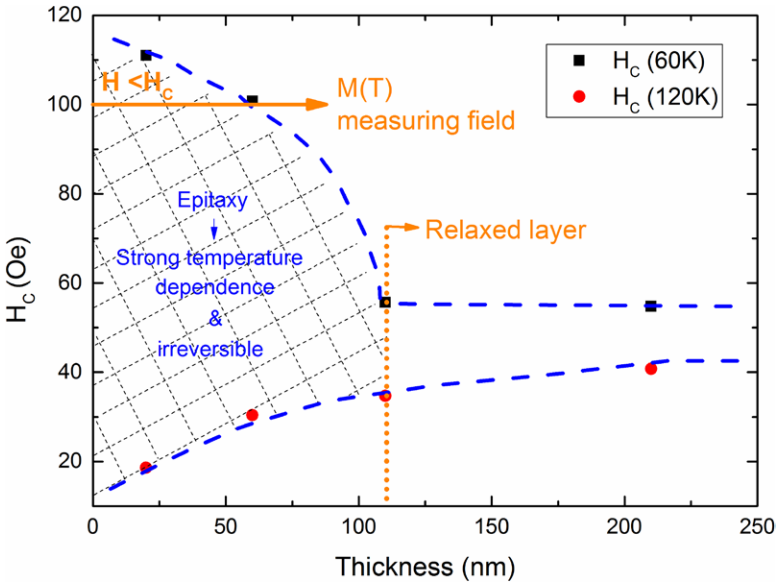


**Figure 5.** Thickness dependence of the coercive field measured at 60 and 120 K.

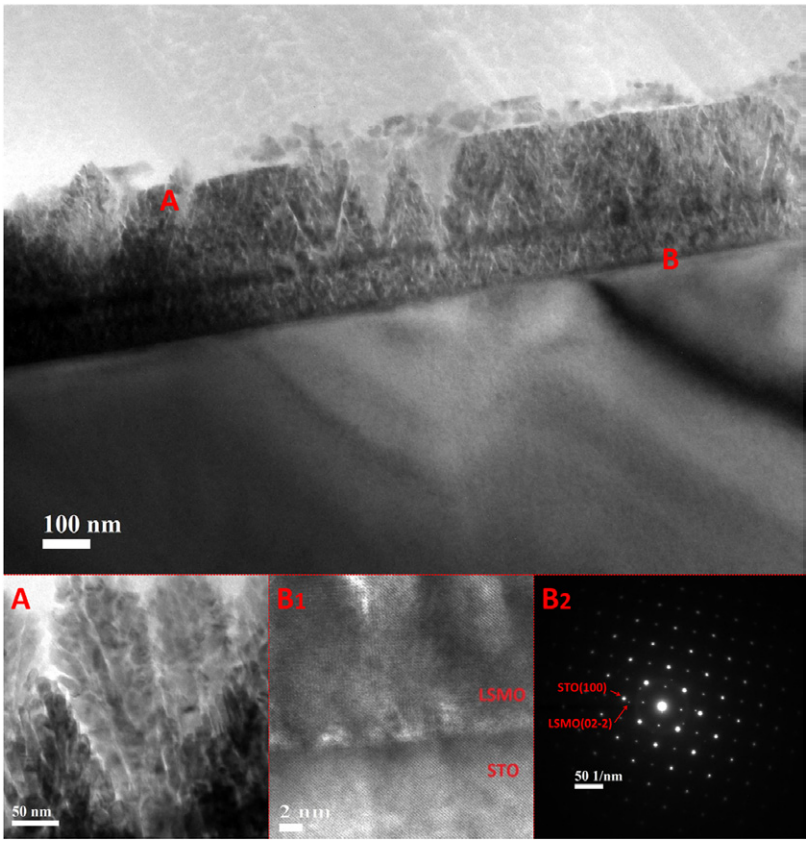


**Figure 6.** HRTEM picture of a cross-sectional sample of 330 nm LSMO thin film deposited on STO substrate. (*a*) Top layer showing a columnar structure caused by the relaxation of the film; (B1) high magnification TEM image and (B2) electron diffraction pattern of the STO/LSMO interface.

substrate (see inset B1), and another that is not directly linked to the substrate and where the film shows a columnar structure (see inset A) associated with relaxation processes, also observed in our XRD analysis and in previous studies [22, 23]. The brighter reflections on the electron diffraction pattern (inset B2 of figure 6) are attributed to STO substrate and the others belong to LSMO film. From the analysis of these reflections, an epitaxial growth LSMO $(0\,2\,-2)\,\|\,$STO $(1\,0\,0)$ relation could be inferred.

The effect of the antiferrodistortive phase transition occurring in the STO substrate changes the other physical properties of the films. The electric resistivity and magnetoresistance

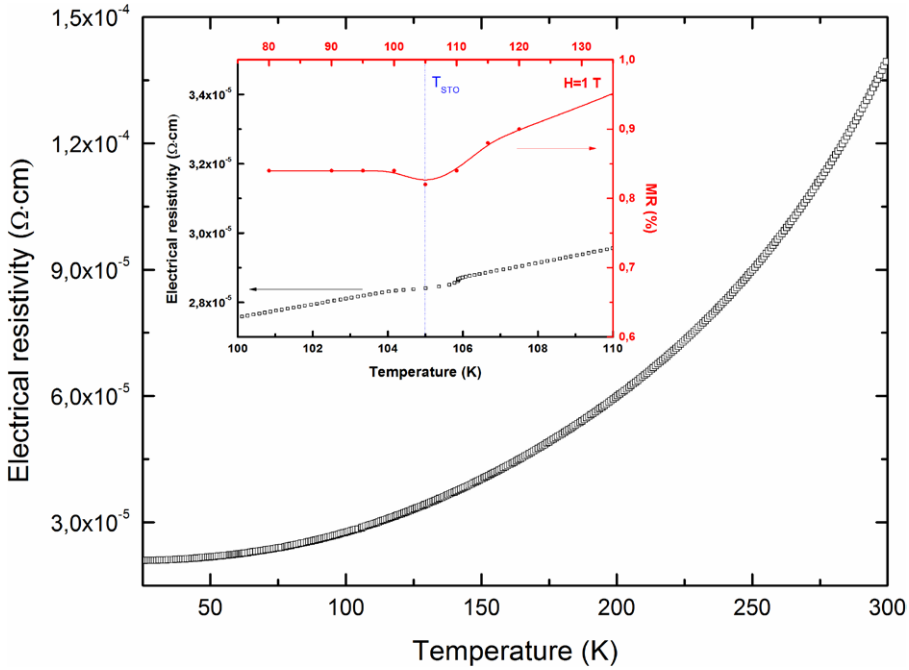


**Figure 7.** Temperature dependence of the electric resistivity of the 60 nm LSMO thin film. The inset shows a zoom image of the electrical resistivity and magnetoresistance close to the $T_{STO}$ of the 60 nm LSMO thin film measured under a magnetic field of 1 T applied parallel to the electrical current and along the [1 0 0] in-plane direction.

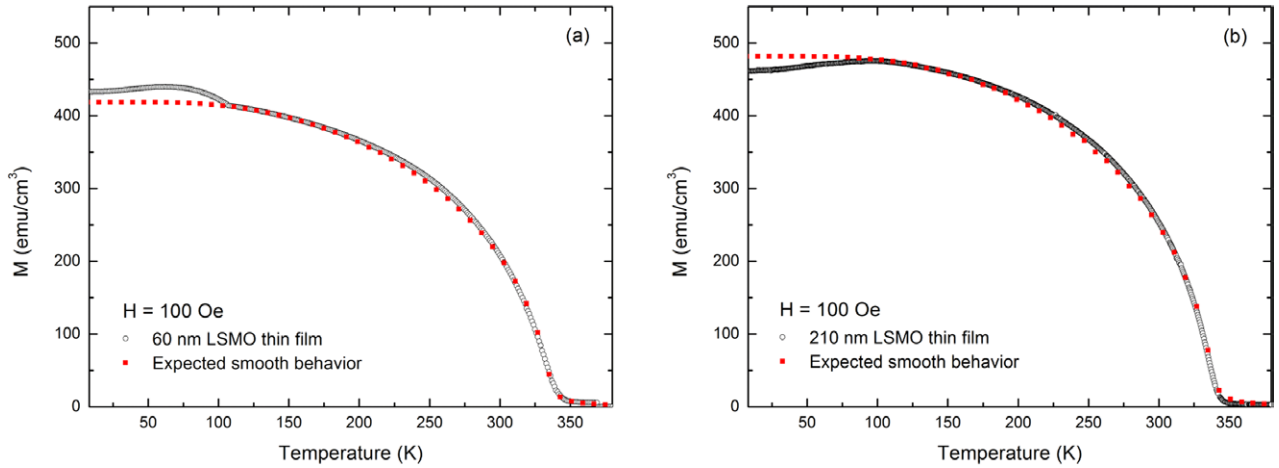


**Figure 8.** Temperature dependence of the 60 nm (*a*) and 210 nm (*b*) LSMO thin film magnetization, measured in field-cooling conditions with 100 Oe applied magnetic field in-plane. The expected smooth behaviour dots are obtained from a simulated Brillouin-like curve.

curves present an anomaly at $T_{STO}$ = 105 K, as shown in the representative figure 7, which demonstrate that they are sensitive to domain wall scattering and corroborates that the anomalous behaviour of the temperature dependence of the coercivity is a genuine effect of the stabilization of the antiferrodistortive phase of the STO substrate below $T_{STO}$=105 K.

Is it well established that the magnetization, measured as a function of temperature, is very sensitive to domain patterns, and more specifically, to the magnetic domain reconfiguration taking place at the antiferrodistortive phase transition occurring at $T_{STO}$. This is particularly important as the pinning between the magnetic domains with the substrate, which induces strain in the film, can modify the film coercivity [24]. Figures 8(*a*) and (*b*) show the dc magnetization for the 60 nm and 210 nm LSMO film, respectively, measured after field cooling the sample under an applied magnetic field of 100 Oe, parallel to the film plane. The temperature dependence of the dc magnetization, recorded above 110 K, follows a smooth behaviour as shown by the auxiliary red dots in figures 8(*a*) and (*b*). These dots are obtained from fitting a Brillouin like curve to the experimental results, which is not actually a Brillouin curve. In fact, the applied magnetic field is below the saturation value, and thus the system is not in thermodynamic equilibrium. The film exhibits a ferromagnetic-like behaviour, with a Curie temperature $T_C$ = 344 K, which is in good agreement with earlier published results [14]. Below $T_{STO}$ = 105 K, the low field magnetization exhibits two distinct anomalous behaviours, starting to deviate from the smooth Brillouin like

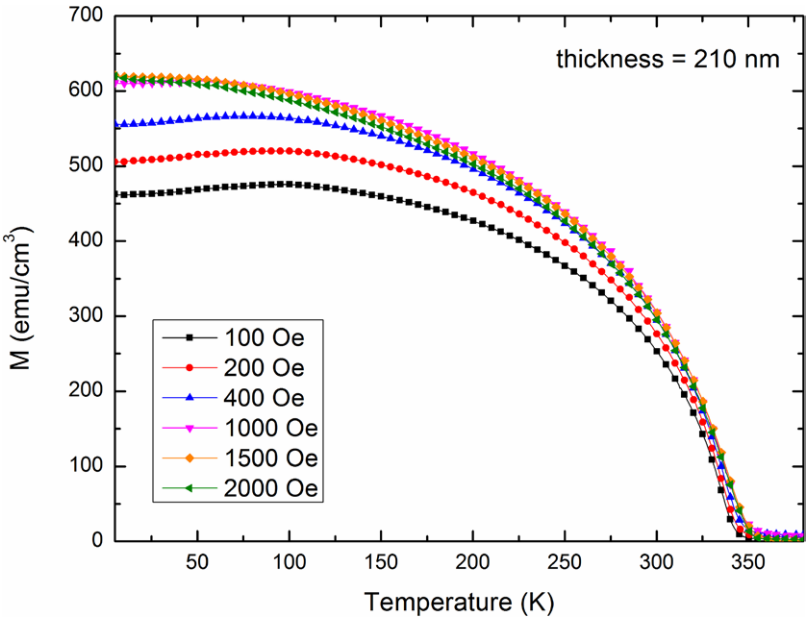


**Figure 9.** Temperature dependence of the magnetization of the 210 nm LSMO thin film measured in field-cooling conditions with different applied in-plane magnetic fields.

curve, depending on the film thickness. We observed that for LSMO thin films with thicknesses up to close to 100 nm have a similar magnetic response to the one shown in figure 8(*a*). In the 60 nm thick film, the magnetic anomaly observed in figure 8(*a*) below $T_{STO}$ is interpreted, as we observed before, by taking into account the epitaxial and coherent film growth which results in the change of the coercive field by a change in film anisotropy. In a similar film thickness, but with a different structure, 2 nm STO/50 nm LSMO thin films, an opposite magnetic behaviour below $T_{STO}$ was observed by Chopdekar *et al* [11]. However, the authors used an applied magnetic field of only 10 Oe, which is below the LSMO coercive field and may not enable a straight comparison with our work.

The magnetic response of the LSMO thin films with thicknesses above 100 nm is similar to the one shown in figure 8(*b*). As we have concluded before and observed by the HRTEM analysis, the impact of the substrate-induced changes is smaller in thicker films which is associated with strain relaxation and to the presence of two different 'layers'. The emergence of an in-defect magnetization could be understood by bringing into discussion magnetic domain reconstructions of the soft LSMO matrix coming from the upper relaxed 'layer' among other plastic defects observed in HRTEM analysis. It is worth noting that this reconstruction of magnetic domains was also proposed by Pesquera *et al* [14]. The 'in-excess' and 'in-defect' magnetizations refer to non-thermodynamic equilibrium magnetic deviations from the expected Brillouin behaviour observed at $T_{STO}$, when magnetic fields below the saturation value are used. In this regard, this terminology refers only to low field magnetizations. Such deviations are associated with distinct magnetic domain patterns created by the clamping to the substrate for low film thicknesses and by the film strain relaxation for higher film thicknesses, as the $M(H)$ experiments clearly confirmed.

It is important to stress that the applied magnetic field used in the $M(T)$ measurements presented here, has a magnitude of 100 Oe, which is below the saturation field (see figure 4), and thus is not sufficiently high to reach full reorientation of the spins. As the magnetization of the LSMO thin films is mostly in the film plane for this field magnitude, we have mainly focused our attention on the results of the magnetization measurements with the applied magnetic field in this direction. Figure 9 shows the $M(T)$ curves for the 210 nm thick film for several applied magnetic fields. Whereas the in-defect magnetization continuously decreases as the magnetic field rises from 100 to 400 Oe; already above a magnetic field of 400 Oe, a thermodynamic state is reached where the magnetization follows a typical Brillouin behaviour. Increasing the magnetic field above the saturation value leads to the one direction orientation of all magnetic domains and consequently the anomalous magnetic behaviour observed below $T_{STO}$ is suppressed.

## 4. Conclusions

This work evidences that antiferrodistortive ordering emerging in STO below 105 K, induces significant changes on the magnetic microstructure of the LSMO thin films. This is specially remarkable in thin films, thinner than 100 nm, due to the lack (or rather smaller) density of plastic defects, among others associated with the strain relaxation, and due to the strong pinning of the magnetic domains of the LSMO film to the substrate domain pattern. These magnetic changes are most evident in the field cooling magnetization and in the coercivity, which largely increases when lowering the temperature below $T_{STO}$. On the contrary, the in-defect magnetization observed for thicker films can be understood

by the formation of randomly oriented magnetic domain reconstructions associated with film relaxations confirmed by both XRD and HRTEM. A full suppression of the anomalous magnetization occurs for high enough applied magnetic fields, wherein a thermodynamic equilibrium is reached. The temperature dependence of the magnetization then follows the usual Brillouin behaviour.

## Acknowledgments

This work was supported by the Fundação para a Ciência e Tecnologia and COMPETE/QREN/EU, through the project PTDC/CTM/099415/2008. The authors are very grateful to Maria João Pereira and Maria Rósario Soares from CICECO, University of Aveiro, for the HR-XRD measurements and discussion of the results. F Figueiras acknowledges FCT grant SFRH/BPD/80663/2011. The authors also acknowledge Projeto Norte-070124-FEDER-000070 and Professor J Fontcuberta for their fruitful discussions.

## References

[1] Millis A J 1998 *Nature* **392** 147
[2] Salamon M B and Jaime M 2001 *Rev. Mod. Phys.* **73** 583
[3] Coey J M D, Viret M and von Molnár S 1999 *Adv. Phys.* **48** 167
[4] Edwards D M 2002 *Adv. Phys.* **51** 1259
[5] Rini M, Tobey R, Dean N, Itatani J, Tomioka Y, Tokura Y, Schoenlein R W and Cavalleri A 2007 *Nature* **449** 72
[6] Xu J, Park J H and Jang H M 2007 *Phys. Rev.* B **75** 012409
[7] Hong J, Stroppa A, Íñiguez J, Picozzi S and Vanderbilt D 2012 *Phys. Rev.* B **85** 054417
[8] Mochizuki M and Furukawa N 2009 *Phys. Rev.* B **80** 134416
[9] Mochizuki M and Furukawa N 2010 *Phys. Rev. Lett.* **105** 187601
[10] Miniotas A, Vailionis A, Svedberg E B and Karlsson U O 2001 *J. Appl. Phys.* **89** 2134
[11] Chopdekar R V, Arenholz E and Suzuki Y 2009 *Phys. Rev.* B **79** 104417
[12] Hayward S A and Salje E K H 1999 *Phase Transit.* **68** 501
[13] Segal Y, Garrity K F, Vaz C A F, Hoffman J D, Walker F J, Ismail-Beigi S and Ahn C H 2011 *Phys. Rev. Lett.* **107** 105501
[14] Pesquera D, Skumryev V, Sánchez F, Herranz G and Fontcuberta J 2011 *Phys. Rev.* B **84** 184412
[15] Ziese M, Vrejoiu I. Setzer A, Lotnyk A and Hesse D 2008 *New J. Phys.* **10** 063024
[16] Egilmez M, Saber M M, Fan I, Chow K H and Jung J 2008 *Phys. Rev.* B **78** 172405
[17] Dagotto E, Hotta T and Moreo A 2001 *Phys. Rep*. **344** 1
[18] de Sousa P 2011 Manganite based magnetoresistive ceramics–$La1_{-x}Sr_xMnO_3$ *MSc Thesis* University of Aveiro, Portugal
[19] Holy V, Pietsch U and Baumbach T 2004 High resolution x-ray scattering *Tracts in Modern Physics* 2nd edn, eds G H Karlsruhe *et al* (Berlin: Springer)
[20] Hibble S J, Cooper S P, Hannon A C, Fawcett I D and Greenblatt M 1999 *J. Phys.: Condens. Matter* **11** 9221
[21] Ranno L, Llobet A, Tiron R and Favre-Nicolin E 2002 *Appl. Surf. Sci.* **188** 170
[22] Pailloux F, Lyonnet R, Maurice J-L and Contour J-P 2001 *Appl. Surf. Sci.* **177** 263
[23] Maurice J-L, Pailloux F, Barthélémy A, Durand O, Imhoff D, Lyonnet R, Rochere A and Contour J-P 2003 *Phil. Mag.* **83** 3201
[24] Blundell S 2001 *Magnetism in Condensed Matter* (New York: Oxford University Press)